

Study on loss processes in solar cells

Ahmed B Abdurrrhman, Fatima Zakria, Hamed A. Said

Department of Electrical and Electronic Engineering, Faculty of Engineering Sciences and Technology, Sebha University, Libya

Keywords:

Photovoltaic (PV)
Intrinsic Losses
Extrinsic Losses
Full Thermal Model FTM

ABSTRACT

Determining heat sources for solar cells is essential to avoid energy loss, which in turn causes the efficiency of solar cells to decrease and therefore, the loss processes have a significant impact on solar conversion. This paper presents a study of intrinsic and exogenous losses in solar cells, identification of the resulting energy loss at different temperatures, and discusses the impact of exogenous and spectral reflectivity on solar cell performance. The results show an increase in thermal loss with an increase in temperature, which in turn leads to a decrease in the efficiency of solar cells. Also explained that the external radiate efficiency, spectral reflectance and operating temperature significantly affect the loss processes. The efficiency of the cell begins to decrease with the decrease of its external radiate efficiency.

دراسة الفقد في الخلايا الشمسية

احمد بوسيف عبد الرحمن، فاطمة زكريا، حامد عبد الحق سعيد

قسم الهندسة الكهربائية والإلكترونية، كلية العلوم الهندسية والتقنية، جامعة سبها، ليبيا

الكلمات المفتاحية:

Photovoltaic (PV)
Intrinsic Losses
Extrinsic Losses
Full Thermal Model FTM

المخلص

تحديد مصادر الحرارة للخلايا الشمسية يعد أمراً ضرورياً لتجنب فقدان الطاقة الذي بدوره يسبب في خفض كفاءة الخلايا الشمسية ومن ثم، فإن عمليات الفقد لها تأثير كبير في التحويل بالطاقة الشمسية. تقدم هذه الورقة دراسة للخسائر الجوهرية والخارجية في الخلايا الشمسية وتحديد فقدان الطاقة الناتج عند درجات حرارة مختلفة كما تناقش تأثير الكفاءة الإشعاعية الخارجية والانعكاسية الطيفية على أداء الخلية الشمسية. وتظهر النتائج زيادة الفقد الحراري مع زيادة درجة الحرارة التي بدورها تؤدي إلى خفض كفاءة الخلايا الشمسية، كما أوضحت أن الكفاءة الإشعاعية الخارجية، والانعكاسية الطيفية ودرجة حرارة التشغيل تؤثر بشكل كبير على عمليات الفقدان، وتبدأ كفاءة الخلية بالانخفاض مع انخفاض كفاءتها الإشعاعية الخارجية.

Introduction

Solar energy photovoltaic technology has developed rapidly for the past years and researchers over the world have been working hard on improving the efficiency and reducing the cost of photovoltaic devices. We constantly see new records of solar photovoltaic (PV) cell efficiencies, which are approaching the theoretical limits. However, the efficiency of photovoltaic devices grows slowly in recent years [1], [2].

Many studies have been conducted on the factors that limit the efficiency of photovoltaic devices. In 1996, Shockley and Queasier developed the first detailed model for ideal solar cells that illustrated the mechanisms of intrinsic (internal) loss called the detailed equilibrium model [3]. Moreover, in 1980, proposed Henry a graphical method for understanding intrinsic losses [4], and in the same year, Wurfel published thermodynamic limitations of solar energy conversion based on the second law of thermodynamics, which is theoretically the highest efficiency of photovoltaic devices

[5]. Later on, studies were carried out to investigate the coefficients of crystalline silicon radiate recombination [6] and Auger recombination [7]. Hirst studied five mechanisms of quantum intrinsic losses and gave a mathematical and graphical demonstration [8]. One year later, Auger recombination was quantified with an improved Model [9]. In addition, the intrinsic losses model for single-junction solar cells was applied but this time considering the AM1.5g standard solar spectrum as the incident power [10]. As in 2015, the Non-Radiate-Recombination processes are considered in the analysis [11]. A year later, was developed full thermal model based on explicit formulas for calculating heat sources, and optical losses and internal processes of solar cells under any incident spectral irradiation [12]. The SQ limit is studied for ideal solar cells but this time using monochromatic light [13]. and has recently introduced an extension of the Full thermal model to evaluate the PV devices [1]. As full thermal model was applied to a bifacial hetero junction solar cell in

*Corresponding author:

E-mail addresses: Ahm.ishteewi@sebhau.edu.ly, (F. Zakria) Fa.zakrya@sebhau.edu.ly, (H. A. Said) Hmdhsd54@gmail.com

Article History : Received 24 December 2020 - Received in revised form 13 February 2021 - Accepted 24 February 2021

2019 [14].

This paper studies the loss processes in photovoltaic devices depending on different kinds of parameters, such as external radiate efficiency(ERE), spectral reflectance, and operating temperature. Energy distributions of a crystalline silicon(c-Si) solar cell are presented to characterize the intrinsic and extrinsic losses in detail, calculated by a thermal model based on the model proposed by Dupré et al [12].

METHODOLOGY

Loss processes in solar cells consist of two parts: intrinsic losses (fundamental losses) and extrinsic losses. Intrinsic losses are unavoidable in single bandgap solar cells, even if in the idealized solar cells [8]. In this paper, this loss was determined based on the full thermal model (FTM) which includes the main loss mechanisms inside the cell and they are in detail explained in [1], [12]. In Table 1, briefly the explicit formulas to calculate different mechanisms and losses at Maximum Power Point (MPP), where the heat sources are represented as “Q” and non-heat sources as “P” ..

Table 1: Explicit formulas of FTM.

Mechanism	Explicit Formula
Reflection	$P_{reflection} = \int_0^{\infty} R_c PFD(E) E dE$
Below E_g	$Q_{belowg} = \int_0^{E_g} (1 - R_c - T_c) PFD(E) E dE$
Thermalization	$Q_{thermalization} = \int_{E_g}^{\infty} (1 - R_c - T_c) PFD(E) (E - E_g) dE$
Carnot	$Q_{carnot} = E_g (1 - \frac{T_a}{T_s})$
Angle Mismatch	$Q_{angle mismatch} = J_{MPP} (\frac{k T_a}{q}) \ln (\frac{\Omega_{emit}}{\Omega_{abs}})$
RR - Emission	$P_{emissionMPP} = E_g J_{emissionMPP}$
NRR Voltage Drop	$Q_{NRRV} = J_{MPP} (\frac{k T_a}{q}) \ln (\frac{1}{ERE_{MPP}})$
NRR Current Drop	$Q_{NRRJ} = E_g (\frac{1}{ERE_{MPP}} - 1) J_{emissionMPP}$
Transport	$Q_{transport} = R_s J_{MPP}^2$
Shunt	$Q_{shunt} = \frac{E_g}{q} (\frac{V_{MPP} + J_{MPP} R_s}{R_{sh}})$
Electrical Power	$P_{MPP} = V_{MPP} J_{MPP}$
The total heat	$Q_{Heat} = Q_{belowg} + Q_{thermalization} + Q_{carnot} + Q_{(angle mismatch)} + Q_{NRRV} + Q_{NRRJ} + Q_{transport} + Q_{shunt}$

The model was applied of crystalline silicon(c-Si) solar cell with the bandgap of 1.1246 eV, under an AM1.5 solar illumination (photon flux density =1000.25 W/m2)The maximum output current and voltage density was determined numerically using:

$$J(V) = J_{sc,Max} - \frac{1}{ERE} J_{emission} \exp\left(\frac{q(V + JR_s)}{kT_a}\right) - \frac{V + JR_s}{R_{sh}} \quad (1)$$

Where Jemit refers to the photocurrent loss caused by radiative recombination, defined as:

$$J_{emission} = \frac{2q\Omega_{emit}}{c^2 h^3} (E^2 kT_a + 2Ek^2 T_a^2 + 2k^3 T_a^3) \exp\left(\frac{qV - E}{kT_a}\right) \quad (2)$$

To discuss the intrinsic losses of solar cells quantitatively, the reflectance R_c and the transmittance T_c of the cell are set to zero, ERE is set to 1, and resistances of the cell (R_s and R.sh) are ignored. Then eq. (1) is written as:

$$J(V) = J_{sc,Max} - \frac{1}{ERE} J_{emission} \exp\left(\frac{q(V)}{kT_a}\right) \quad (3)$$

Fig. 1 shows the equivalent circuit diagram of a solar cell. By taking all loss processes into consideration, eq. (1) is used to derive the necessary parameters. Firstly, V_MPP and J_MPP are calculated by finding the maximum power point (P_MPP = [J_MPP V]_MPP) with the variables imposed R_s=1.1 Ω [cm] ^2, R_sh=240 Ω [cm] ^2, T_c=0, T_s=5800 K, Ω_emit=π, Ω_abs=Ω_emit/46200, and cases of different EREs (ERE= [10] ^(-1), ERE= [10] ^(-5)) are calculated to illustrate the impact of external radiate efficiency on loss processes at different temperatures, as well R_c=0.1, R_c=0.05 to illustrate the effect of spectral reflectance on cell performance.

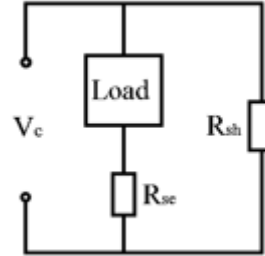


Fig. 1. Equivalent circuit diagram of a solar cell showing the load, series resistance (R_s), shunt resistance (Rsh) and the voltage across the cell (V_c).

Results and discussion

The results in Table 2 and Fig. 2 indicate the fundamental (basic) losses that they take up the majority of the incident energy, and that a large amount of solar energy is converted into heat. The efficiency of the ideal crystalline silicon cell (ERE=1) is achieved 33.52% at a temperature 298.15 K. The relative error is

$$\delta = (|P_{Output} + P_{Heat} + P_{Emission} - P_{Incident}|) / P_{Incident}. \quad (4)$$

The total of energy distributions expressed in this equation agree well with the incident solar energy, which prove the model of high accuracy.

Table 2 Energy distribution and corresponding parameters of a c-Si solar cell

crystalline silicon solar cell, $E_g=1.1246$ eV, $T_a=298.15$ k, $ERE=1$				
	Current	Voltage	Power	/P _{Incident}
	A/m ²	V	W/m ²	%
$J_{sc}/V_{msc}/P_{Incident}$	436.40	1.1246	1000.25	100
Q_{Below}			194.34	19.45
$Q_{Thermalization}$			315.35	31.51
$P_{Emission}$	13.13		14.76	1.47
Q_{Carnot}		0.0578	24.45	2.44
Q_{Angle}		0.276	116.80	11.68
P_{Output}	$J_{MPP}=423.27$	$V_{MPP}=0.792$	335.24	33.52(η)
Δ	0	0	-0.6	0
Q_{Heat}	650.94			65.07

At room temperature.

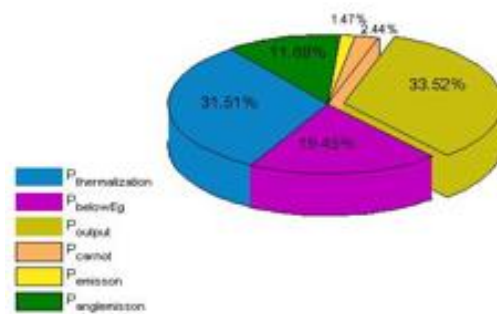


Fig. 2. Energy distributions of a c-Si solar cell at room temperature.

Fig. 3 shows the effect of external radiation efficiency on the efficiency of solar cells below the solar spectrum (AM1.5) at a

temperature (298.15) as the highest efficiency obtained at ERE=1 and cell efficiency begins to decrease with lower external radiate efficiency. Fig. 4 shows the distribution of fallen solar energy (imposing black body radiation at 5800 k) at different external radiate efficiency with the bandgap, the larger the bandgap, the smaller the heat source and the fewer loss processes associated with radiation re-union with increased band gap and increased external radiate efficiency. From Table 3 for external radiate efficiency it does not affect loss processes except for NRR loss where NRR_V= 2.07% at ERE= 10^{-1} and 10.44% at ERE= 10^{-5} and At ERE= 2.22×10^{-7} is 13.75% and this excess energy is converted to heat, which reduces cell efficiency as a result.

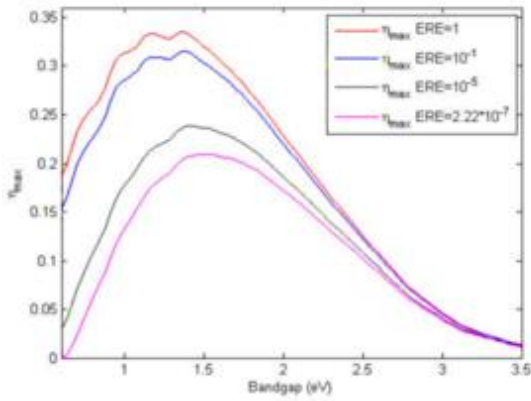


Fig. 3. Efficiency of ideal solar cells only considering the intrinsic losses at different external radiate efficiency at room temperature.

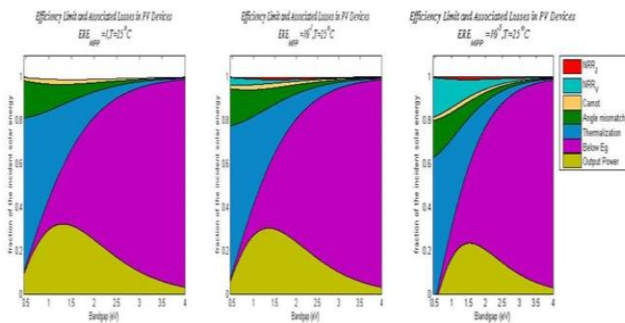


Fig. 4. Energy distribution of solar cells in radiate limit at room temperature. The external radiate efficiency are ERE=1 in (a), ERE=10-1 in (b), ERE=10-5 in (c), respectively.

The results in the Table 4, Table 5 and the fig.5 ,fig. 6 showed that an increase in the temperature of the cell leads to a decrease in its efficiency from 16.68% at room temperature to 14.58% at 55° at the radiative limit ERE= 10^{-5} , and from 24.4% at room temperature to 23.1% at 55° at the radiative limit ERE= 10^{-1} . Also showed the increase in the amount of heat generated from 705.12 W m⁻² at room temperature to 760.81 W m⁻² at 55°. This is humiliating that the amount of heat is directly proportional to the high temperature and inversely to external radiate efficiency (ERE) . To study the effect of spectral reflectance on the performance of the solar cell, the results shown in Table 6 and fig. 7 show an increase in efficiency from 24.4% at R_c=0.1 to 25.85% at R_c = 0.05 in room temperature, this increase is a decrease in the process of loss of the current by reflection from 43.64 (A/m²) at R_c=0.1 to 21.82 A/m² at R_c=0.05.

Table 3 Energy distribution and corresponding parameters of a c-Si solar cell with different external radiate efficiency at room temperature.

crystalline silicon solar cell, $E_g=1.1246$ eV, $T_a=298.15$ K												
	ERE= 10^{-1}				ERE= 10^{-5}				ERE= 2.22×10^{-7}			
	Current	Voltage	Power	$\beta_{Incident}$	Current	Voltage	Power	$\beta_{Incident}$	Current	Voltage	Power	$\beta_{Incident}$
Units	A/m ²	V	W/m ²	%	A/m ²	V	W/m ²	%	A/m ²	V	W/m ²	%
$J_{ph}/V_{oc}/P_{Incident}$	436.4	1.124	1000.25	100	436.4	1.124	1000.25	100	436.4	1.124	1000.25	100
$P_{Reflection}$	43.64		100.0	10.00	43.64		100.0	10.00	43.64		100.0	10.00
P_{Below}			174.9	17.49			174.9	17.49			174.9	17.49
$P_{Thermalization}$			283.81	28.38			283.81	28.38			283.8	28.38
$P_{Emission}$	1.11		1.24	0.12	0		0	0	0		0	0
P_{Carnot}		0.057	20.29	2.02		0.051	20.40	2.04		0.057	20.18	2.01
P_{Angle}		0.276	96.91	9.69		0.276	97.46	9.74		0.276	96.40	9.64
P_{NRR-J}	10.01		11.24	1.12	18.42		20.71	2.07	25.79		29.20	2.92
P_{NRR-V}		0.059	20.77	2.07		0.295	104.47	10.44		0.393	137.51	13.75
P_{Series}		0.035	12.33	1.23		0.0353	12.47	1.24		0.034	12.20	1.22
P_{Shunt}	30.47		34.25	3.43	21.15		23.77	2.37	17.44		19.60	1.96
P_{Output}	JMPP =351.17	VMPP =0.696	244.48	24.44 (η)	JMPP =353.18	VMPP =0.472	166.81	16.68(η)	JMPP =349.34	VMPP =0.383	134.04	13.40(η)
Δ	0	0	0.03	0	0.01	0	-4.5	-0.45	0.19	-0.01	-7.6	0.76
P_{Heat}			654.5	65.4			705.12	70.51			773.79	77.37

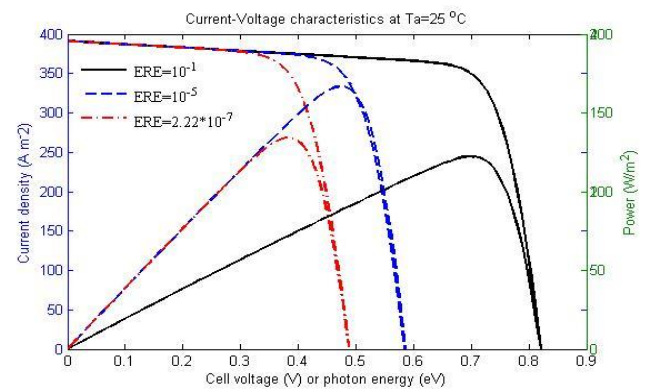


Fig. 5. Voltage-current curve of the solar cell at different external radiative efficiencies.

Table 4 Energy distribution and corresponding parameters of a c-Si solar cell with external radiate efficiency (ERE)=10-1 at different temperatures.

crystalline silicon solar cell, $E_g=1.1246$ eV												
	ERE= 10^{-1}											
	$T_a=308.15$ K				$T_a=318.15$ K				$T_a=328.15$ K			
	Current	Voltage	Power	$\beta_{Incident}$	Current	Voltage	Power	$\beta_{Incident}$	Current	Voltage	Power	$\beta_{Incident}$
Units	A/m ²	V	W/m ²	%	A/m ²	V	W/m ²	%	A/m ²	V	W/m ²	%
$J_{ph}/V_{oc}/P_{Incident}$	436.4	1.124	1000.25	100	436.4	1.124	1000.25	100	436.4	1.124	1000.25	100
$P_{Reflection}$	43.64		100.0	10.00	43.64		100.0	10.00	43.64		100.0	10.00
P_{Below}			174.9	17.49			174.9	17.49			174.9	17.49
$P_{Thermalization}$			283.1	28.31			283.1	28.31			283.1	28.31
$P_{Emission}$	1.31		1.4	0.14	0.43		0.48	0.04	0.40		0.44	0.04
P_{Carnot}		0.059	20.8	2.08		0.061	21.4	2.14		0.063	22.2	2.22
P_{Angle}		0.285	99.6	9.96		0.294	102.3	10.23		0.303	106.3	10.63
P_{NRR-J}	11.87		13.3	1.33	13.93		15.6	1.56	12.41		13.9	1.39
P_{NRR-V}		0.061	21.3	2.13		0.063	21.9	2.19		0.059	22.7	2.27
P_{Series}		0.035	12.2	1.22		0.0348	12.08	1.20		0.035	12.25	1.22
P_{Shunt}	30.08		33.8	3.38	29.67		33.35	3.33	28.95		32.55	3.25
P_{Output}	JMPP =349.5	VMPP =0.686	240.03	24.0 (η)	JMPP =347.6	VMPP =0.677	235.47	23.54(η)	JMPP =350.01	VMPP =0.66	231.02	23.10(η)

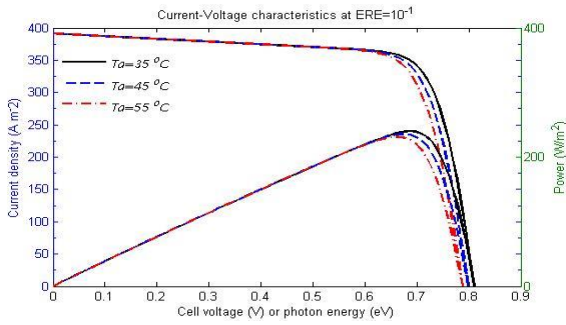


Fig. 6. Voltage-current curve of the solar cell with external radiate efficiency (ERE)=10-1 at different temperatures.

Table 5 Energy distribution and corresponding parameters of a c-Si solar cell with external radiate efficiency (ERE)=10-5 at different temperatures.

crystalline silicon solar cell, $E_g=1.1246$ eV													
ERE=10 ⁻⁵													
Ta=328.15 K				Ta=328.15 K				Ta=328.15 K					
Units	Current	Voltage	Power	$P_{Incident}$	Current	Voltage	Power	$P_{Incident}$	%	Current	Voltage	Power	$P_{Incident}$
	A/m ²	V	W/m ²	%	A/m ²	V	W/m ²	%	%	A/m ²	V	W/m ²	%
$J_{ph}/V_{max}/P_{Incident}$	436.4	1.124	1000.25	100	436.4	1.124	1000.25	100	436.4	1.124	1000.25	100	436.4
$P_{Reflection}$	43.64		100.0	10.00	43.64		100.0	10.00	43.64		100.0	10.00	43.64
P_{Below}			174.9	17.49			174.9	17.49			174.9	17.49	
$P_{Thermalization}$			283.1	28.31			283.1	28.31			283.1	28.31	
$P_{Emission}$	0		0	0	0		0	0	0		0	0	0
P_{Carnot}		0.059	20.8	2.08		0.061	21.5	2.15			0.063	22.2	2.22
P_{Angle}		0.285	99.6	9.96		0.294	102.9	10.29			0.303	106.1	10.63
P_{NRR-J}	22.96		25.8	2.58	23.47		26.3	2.63	24.34		27.36	2.73	
P_{NRR-V}		0.305	106.7	10.67		0.315	110.3	11.03			0.325	113.8	11.38
P_{Series}		0.035	12.2	1.22		0.0348	12.08	1.20			0.035	12.25	1.22
P_{Shunt}	20.49		23.03	2.30	19.62		22.06	2.20	18.77		21.1	2.11	
P_{Output}	JMPP =349.3	VMPP =0.457	159.62	15.95	JMPP =349.66	VMPP =0.436	152.48	15.24(η)	JMPP =349.64	VMPP =0.415	145.34	14.53(η)	
Δ	0.01	-0.01	-5.5	-0.56	0.01	-0.01	-5.4	-0.54	0.01	-0.01	-5.9	-0.59	
P_{Heat}			746.13	74.6			753.14	75.3			760.81	76.08	

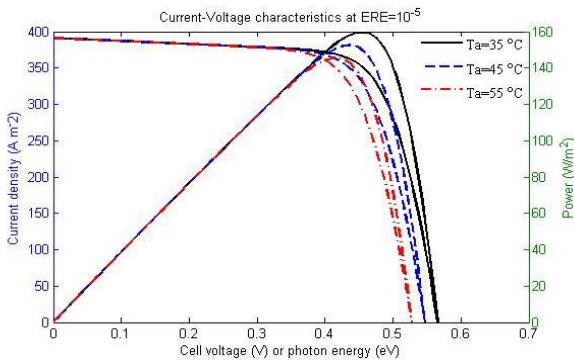


Fig. 7. Voltage-current curve of the solar cell with external radiate efficiency (ERE)=10-1 at different temperatures.

Table 6 Energy distribution and corresponding parameters of a c-Si solar cell with external radiate efficiency (ERE)=10-1 and spectral reflectance (R_c)=0.05 at room temperature.

c-Si solar cell, $E_g=1.1246$ eV				
ERE/Ta/Rc	10 ⁻¹		298.15 k	
	Current	Voltage	Power	$P_{Incident}$
	A/m ²	V	W/m ²	%
$J_{ph}/V_{max}/P_{Incident}$	436.40	1.1246	1000.25	100
$P_{Optical}$	21.82		50.01	5.00
P_{Below}			184.62	18.48
$P_{Thermalization}$			299.58	29.93
$P_{Emission}$	0.29		0.33	0.03
P_{Carnot}		0.057	21.45	2.14
P_{Angle}		0.276	102.47	10.24
P_{NRR-J}	11.42		12.84	1.28
P_{NRR-V}		0.059	21.96	2.19
P_{Series}		0.037	13.78	1.37
P_{Shunt}	30.55		34.34	3.43
P_{Output}	371.33	0.696	258.51	25.85 (η)
Δ	-0.01	0	0.36	0.03
P_{Heat}			691.04	69.08

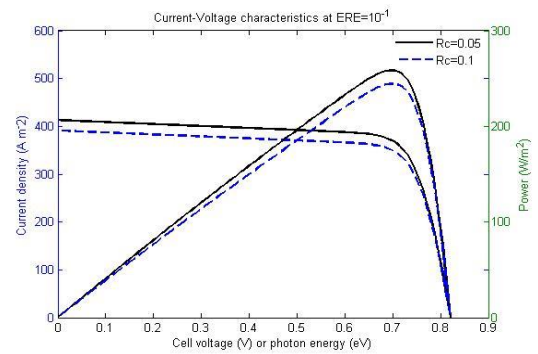


Fig. 8. Voltage-current curve of the solar cell with external radiate efficiency (ERE)=10-1 and spectral reflectance (R_c)=0.05 at room temperature.

Conclusion

This paper study of the intrinsic and external losses in solar cells and the determination of the resulting energy loss at different temperatures. It also discusses the effect of external radiative efficiency and spectral reflectance on the performance of the solar cell. The results show that the processes of loss and temperature increase have a major impact on the efficiency of the solar cell. With the increase of these two factors, the efficiency decreases, and the basic losses processes have the majority of the energy falling and thus the amount of heat more. In addition to the loss processes, the operating temperature and the external radiate efficiency affect the performance of the solar cell.

References

- Wang, A. and Y. Xuan (2018). "A detailed study on loss processes in solar cells." Energy 144: 490-500.
- Green, M. A., et al. (2019). "Solar cell efficiency tables (version 54)." Progress in Photovoltaics: Research and Applications 27(NREL/JA-5K00-74116).
- Shockley, W. and H. J. Queisser (1961). "Detailed balance limit of efficiency of p-n junction solar cells." Journal of Applied Physics 32(3): 510-519.
- Henry, C. H. (1980). "Limiting efficiencies of ideal single and multiple energy gap terrestrial solar cells." Journal of Applied Physics 51(8): 4494-4500.
- Wurfel, P. and W. Ruppel (1980). "Upper limit of thermophotovoltaic solar-energy conversion," IEEE Trans. Electron Devices 27(4): 745-750.
- Trupke, T., et al. (2003). "Temperature dependence of the radiative recombination coefficient of intrinsic crystalline silicon." Journal of Applied Physics 94(8): 4930-4937.
- Kerr M.J, A. Cuevas, and P. Campbell (2003). "Limiting efficiency of crystalline silicon solar cells due to Coulombenhanced Auger recombination," Progress in Photovoltaics: Research and Applications 11(2):97-104.
- Hirst, L. C. and N. J. Ekins-Daukes (2011). "Fundamental losses in solar cells." Progress in Photovoltaics: Research and Applications 19(3): 286-293.
- Richter, A., et al. (2012). "Improved quantitative description of Auger recombination in crystalline silicon." Physical Review B 86(16): 165202.
- M. Jost and M. Topič (2014). "Efficiency limits in photovoltaics: Case of single junction solar cells," Facta universitatis - series: Electronics and Energetics 27(4):631-638.
- Dupré, O., et al. (2015). "Physics of the temperature coefficients of solar cells." Solar energy materials and solar cells 140: 92-100.
- Dupré, O, R. Vaillon, and M. A. Green (2016). "A full thermal model for photovoltaic devices," Solar Energy 140 : 73-82.
- R. Kimovec and M. Topič (2017). "Comparison of measured performance and theoretical limits of gas laser power converters under monochromatic light," Facta universitatis - series: Electronics and Energetics 30(1):93-106.
- Ascencio-Vasquez, J., et al. (2019). Application of the full thermal model for PV devices.